REPORT DOCUMENTATION PAGE

Form Approved
OMB No. 0704-0188

1. REPORT DATE (DD-MM-YYYY)	2. REPORT TYPE	3. DATES COVERED (From - To)
29-Sep-2006	REPRINT	

4. TITLE AND SUBTITLE
TRANSITION ZONE WAVE PROPAGATION: CHARACTERIZING TRAVEL-TIME AND AMPLITUDE INFORMATION

5a. CONTRACT NUMBER
FA8718-06-C-0005

5b. GRANT NUMBER

5c. PROGRAM ELEMENT NUMBER
62601F

6. AUTHOR(S)
Peter M. Shearer and Jesse F. Lawrence

5d. PROJECT NUMBER
1010

5e. TASK NUMBER
SM

5f. WORK UNIT NUMBER
A1

7. PERFORMING ORGANIZATION NAME(S) AND ADDRESS(ES)

University of California San Diego
8602 La Jolla Shores Drive
La Jolla, CA 92093-0210

8. PERFORMING ORGANIZATION REPORT NUMBER

9. SPONSORING / MONITORING AGENCY NAME(S) AND ADDRESS(ES)
Air Force Research Laboratory
29 Randolph Road
Hanscom AFB, MA 01731-3010

10. SPONSOR/MONITOR'S ACRONYM(S)
AFRL/VSBYE

11. SPONSOR/MONITOR'S REPORT NUMBER(S)
AFRL-VS-HA-TR-2006-1114

12. DISTRIBUTION / AVAILABILITY STATEMENT
Approved for Public Release; Distribution Unlimited.

13. SUPPLEMENTARY NOTES
Reprinted from: Proceedings of the 28th Seismic Research Review – Ground-Based Nuclear Explosion Monitoring Technologies, 19 – 21 September 2006, Orlando, FL, Volume I pp 267 - 272.

14. ABSTRACT

We characterize transition-zone seismic wave propagation by mapping and calibrating the travel-time and amplitude behavior of P waves traveling through the transition zone at epicentral distances from 13 to 30 degrees and modeling the triplications resulting from the 410- and 660-km discontinuities. We have built an online database of waveforms from the IRIS FARM archive, which consists of broadband data from the global seismic networks as well as portable seismic arrays deployed in PASSCAL experiments. We process the data to compute source and station amplitude terms to correct for different magnitude sources and near-receiver site effects as well as errors in the instrument response functions. We then compute both global and regional stacks to obtain the average time and amplitude of the wavefield within the 13- to 30-degree distance interval. Because the timing of the secondary branches is variable, we implement an envelope-function stacking method to obtain robust results. We model our data stacks using WKBJ synthetic seismograms and a niching genetic algorithm to explore the model space of different transition-zone velocity structures. We compare these results with long-wavelength models of 410- and 660-km discontinuity topography obtained from SS precursors and more detailed images beneath individual seismic stations derived from receiver functions. Our goal is to produce integrated transition-zone models of seismic velocity and discontinuity topography that will improve our ability to locate and estimate magnitudes of events recorded at regional distances.

15. SUBJECT TERMS
Seismic characterization, Seismic propagation

16. SECURITY CLASSIFICATION OF:			17. LIMITATION OF ABSTRACT	18. NUMBER OF PAGES	19a. NAME OF RESPONSIBLE PERSON
a. REPORT	b. ABSTRACT	c. THIS PAGE			Robert J. Raistrick
UNCLAS	UNCLAS	UNCLAS	SAR	6	19b. TELEPHONE NUMBER (include area code) 781-377-3726

TRANSITION ZONE WAVE PROPAGATION: CHARACTERIZING TRAVEL-TIME AND AMPLITUDE INFORMATION

Peter M. Shearer and Jesse F. Lawrence

University of California San Diego

Sponsored by Air Force Research Laboratory

Contract No. FA8718-06-C-0005

ABSTRACT

We characterize transition-zone seismic wave propagation by mapping and calibrating the travel-time and amplitude behavior of P waves traveling through the transition zone at epicentral distances from 13 to 30 degrees and modeling the triplications resulting from the 410- and 660-km discontinuities. We have built an online database of waveforms from the IRIS FARM archive, which consists of broadband data from the global seismic networks as well as portable seismic arrays deployed in PASSCAL experiments. We process the data to compute source and station amplitude terms to correct for different magnitude sources and near-receiver site effects as well as errors in the instrument response functions. We then compute both global and regional stacks to obtain the average time and amplitude of the wavefield within the 13- to 30-degree distance interval. Because the timing of the secondary branches is variable, we implement an envelope-function stacking method to obtain robust results. We model our data stacks using WKBJ synthetic seismograms and a niching genetic algorithm to explore the model space of different transition-zone velocity structures. We compare these results with long-wavelength models of 410- and 660-km discontinuity topography obtained from SS precursors and more detailed images beneath individual seismic stations derived from receiver functions. Our goal is to produce integrated transition-zone models of seismic velocity and discontinuity topography that will improve our ability to locate and estimate magnitudes of events recorded at regional distances.

OBJECTIVES

This project studies the effects of heterogeneous transition zone structure on seismic travel times and amplitudes. Accurate predictions of P- and S-wave travel times and amplitudes at distances between 13 and 30 degrees are hindered by the sensitivity of the multiple travel-time branches at these distances to variable structure in the mantle transition zone. Both discontinuity topography and bulk seismic velocity anomalies perturb seismic ray paths, which cause focusing and defocusing effects on wave amplitudes as well as travel-time anomalies. However, travel time and amplitude information is critical for locating and estimating magnitudes of target events. By comparing regional variations of triplication amplitudes and travel times with predictions of 3D seismic velocity models, we will obtain improvements in mantle transition zone models, as well as in the estimated locations and magnitudes of recorded events.

The effect of the mantle discontinuities at 410- and 660-km depth is shown in Figure 1, which depicts a series of P-wave ray paths between 13 and 35 degrees. Retrograde branches result from the velocity jump at each of the discontinuities, causing the familiar double triplication centered at about 20 degrees. However, the positions of these branches are sensitive to the discontinuity depths, which typically vary by 30 km or more (e.g., Shearer, 1990, 1991, 1993; Shearer and Masters, 1992; Flanagan and Shearer, 1998a,b; Gu et al., 1998), and to the size of the velocity jumps at the discontinuities, which also exhibit considerable variation (e.g., Melbourne and Helmberger, 1998; Shearer and Flanagan, 1999; Chambers et al., 2005). In addition, there is some sensitivity to 3D velocity variations in the transition zone.

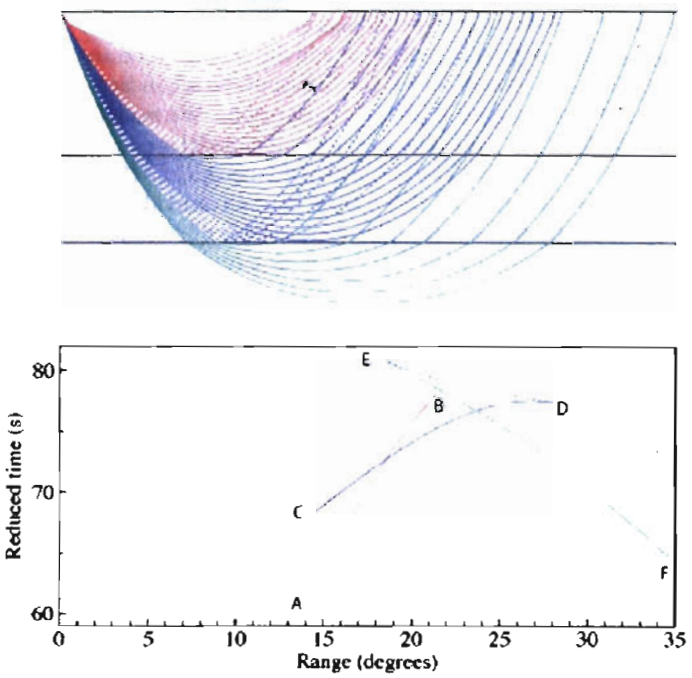

Figure 1. Discontinuities in the mantle transition zone at 410- and 660-km depths cause a pair of triplications in P- and S-wave arrivals between ~15 and 30 degrees. The ray paths (top) are color-coded and correspond to the different branches in the travel-time curve plotted below (reduced at 10 s/degree). The AB branch consists of direct waves that bottom above the 410-km discontinuity (red solid). The BC branch reflects at 410 km (red dashed). The CD and DE branches bottom above and reflect off the 660-km discontinuity (blue solid and dashed). The EF branch bottoms in the lower mantle. This figure is adopted from Shearer (2000).

We plan a series of tests to compare observed P- and S-wave travel times and amplitudes with predictions based on the best current models. These tests will illuminate the strengths and weaknesses of these models and determine if the models are sufficient to explain anomalous travel times and amplitudes at these distances (and consequently

check the robustness of our current event locations and amplitude predictions). This project also will compare global and regional travel-time data sets with thousands of new measurements of travel times and amplitudes recorded at both temporary and permanent seismic stations. These new measurements will focus on obtaining times and amplitudes for all triplication phases, not just the first arrivals. Where data coverage is sufficient, we intend to improve portions of our current models by integrating these new measurements into hybrid models. This will yield more accurate earthquake locations and magnitude estimates for these regions. It may also be possible to interpolate these models to some extent to improve our transition zone models for low data coverage regions.

The triplications cause difficulties for traditional methods of source location, magnitude estimation, and inversions for 3D velocity structure. Therefore, triplication data are typically avoided for seismic tomography and source location. However, details of the triplications can be useful for characterizing heterogeneity and calculating better source locations. With sufficient data, the secondary branches can be used to model variations in discontinuity topography and seismic velocity. Once the structural properties are determined, the high sensitivity of triplication travel-time and amplitude fluctuations to source location and magnitude make triplications ideal for determining source characteristics. However, without an appropriate transition zone model, these times cannot yield accurate times or amplitudes.

The relevance of our results for nuclear test monitoring is that better structural models of transition zone structure will reduce source location and magnitude uncertainties. The anomalous arrival times and amplitudes between 13 and 30 degrees currently limit the usefulness of regional phase data in calculating accurate source locations and event magnitudes. However, records from closer distances are not likely to be available in many parts of the world and small magnitude events are often not well recorded at longer distances because of the sharp drop in P and S amplitudes that occurs just beyond 30 degrees. Thus, unraveling the complexities of the travel-time triplications and improving our models of the transition zone are likely to be critical for accurate monitoring of a significant number of target events.

RESEARCH ACCOMPLISHED

Our initial efforts have concentrated on assembling a database of waveforms from the IRIS FARM archive, which consists of broadband data from the global seismic networks as well as portable seismic arrays deployed in PASSCAL experiments. This involves transferring the data from the IRIS DMC, running the READSEED program to convert them from the SEED format to SAC, and then running a program to convert them to the GFS format that we use for subsequent processing. The GFS files are currently being stored on a RAID system, with both mirroring and tape backup for redundancy in the event of hardware failures. Configuring the RAID system took considerable time, as well as sorting out some of the timing difficulties associated with multiple time windows in the FARM archive, but now we have transferred almost all of the data to our RAID system.

We have also completed computing index files and signal-to-noise estimates for the P and S arrivals, which facilitates later processing and provides a check on the timing integrity of the GFS waveforms. Our basic approach is to measure the signal-to-noise as the ratio between the maximum amplitude (peak to trough) in a time window that contains the phase of interest and a pre-event noise window of equal length. Because the raw data are broadband, we perform this operation separately for different frequency bands.

Finally, we have begun preliminary time and amplitude stacks for the transition zone wavefield and are writing software to isolate station and event correction terms. We also are adapting a WKBJ synthetic seismogram code to generate suites of model predictions for comparison to the data. Our analyses so far have concentrated on characterizing the globally averaged wavefield as a starting reference point for studies of regional variations. Because the position of the triplicated phases is highly variable, we have adopted an envelope-stacking approach that is robust with respect to travel time variations. A simple measure of amplitude versus distance for shallow events (<30 km depth) is provided by the maximum amplitude within a given frequency band. To obtain meaningful results, however, first it is necessary to apply empirical corrections for source size and station gain (or local site effects). We compute these terms iteratively using a robust least-squares method that automatically downweights data outliers.

Results of this analysis for P-waves from earthquakes between 1981 and 2004 are shown in Figure 2, compared to synthetic seismogram predictions for three different models of upper mantle discontinuity depths. Notice that the

amplitude peaks between 15 and 25 degrees as a result of the focusing of energy from the steep velocity gradients through the transition zone. The overall amplitude versus distance behavior is similar to that obtained by Veith and Clawson (1972) for magnitude calibration. Our synthetic seismograms are computed using a WKBJ method, which provides comparable results to reflectivity synthetics at much less computational cost. The advantage of WKBJ is that it will enable us to explore the data fits provided by testing thousands of different models.

The fit between data and synthetics is not perfect and we plan to test whether this reflects limited sampling of model space or a more fundamental problem. In addition to the velocity and Q structure through the transition zone, there are questions regarding exactly how to best filter the data and how to simulate the averaging process (which combines data from many different source-receiver paths and transition zone structures). Our ultimate goal is to perform this modeling separately among different regions.

Some idea of the coverage of the transition zone that we are likely to achieve is shown in Figure 3, which is based on stations and sources contained in the FARM database between 1981 and 2001. The best coverage is in the Middle East and southeastern Asia where it should be possible to completely resolve the mantle triplications.

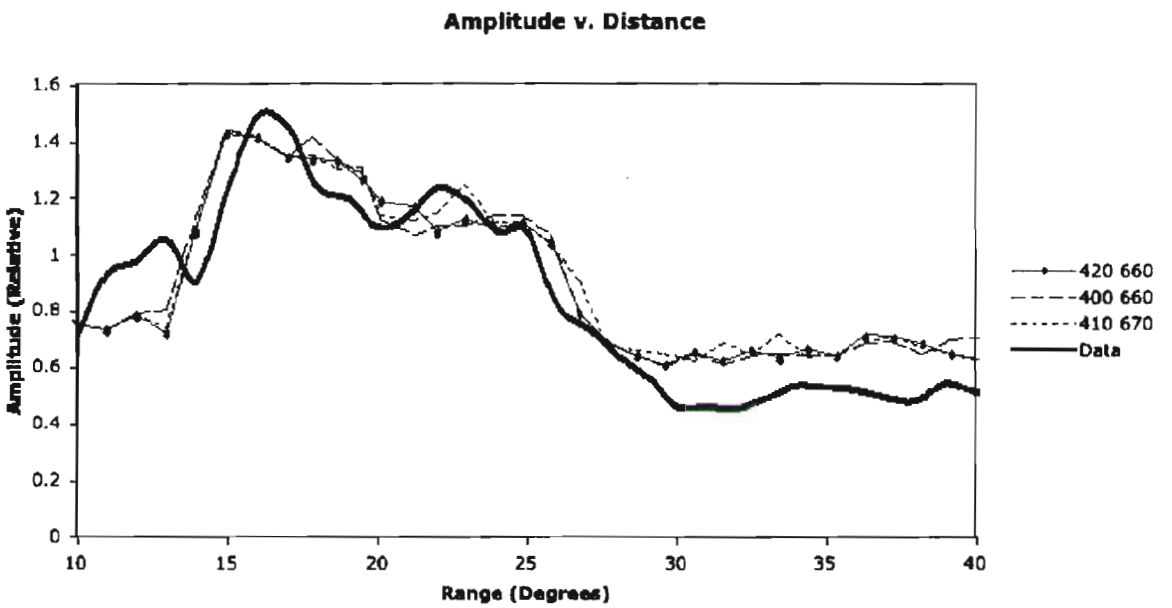

Figure 2. Observed average amplitude versus epicentral distance for shallow earthquakes in the IRIS FARM database. Empirical corrections have been applied for source and station differences. The largest amplitudes occur near 17 degrees and amplitudes are nearly constant beyond 30 degrees.

CONCLUSIONS AND RECOMMENDATIONS

This IRIS FARM database provides a large resource for probing transition zone structure and for characterizing seismic wave propagation through this region at epicentral distances from 13 to 30 degrees. Travel-time and amplitude anomalies reflect large regional differences in upper-mantle discontinuity topography, which can be mapped using synthetic seismograms and compared to long-wavelength models of seismic velocity and discontinuity topography. We anticipate rapid progress on this project now that most of the preliminary data processing and archiving is complete.

ACKNOWLEDGEMENTS

We thank Kris Walker for his work in assembling the FARM database.

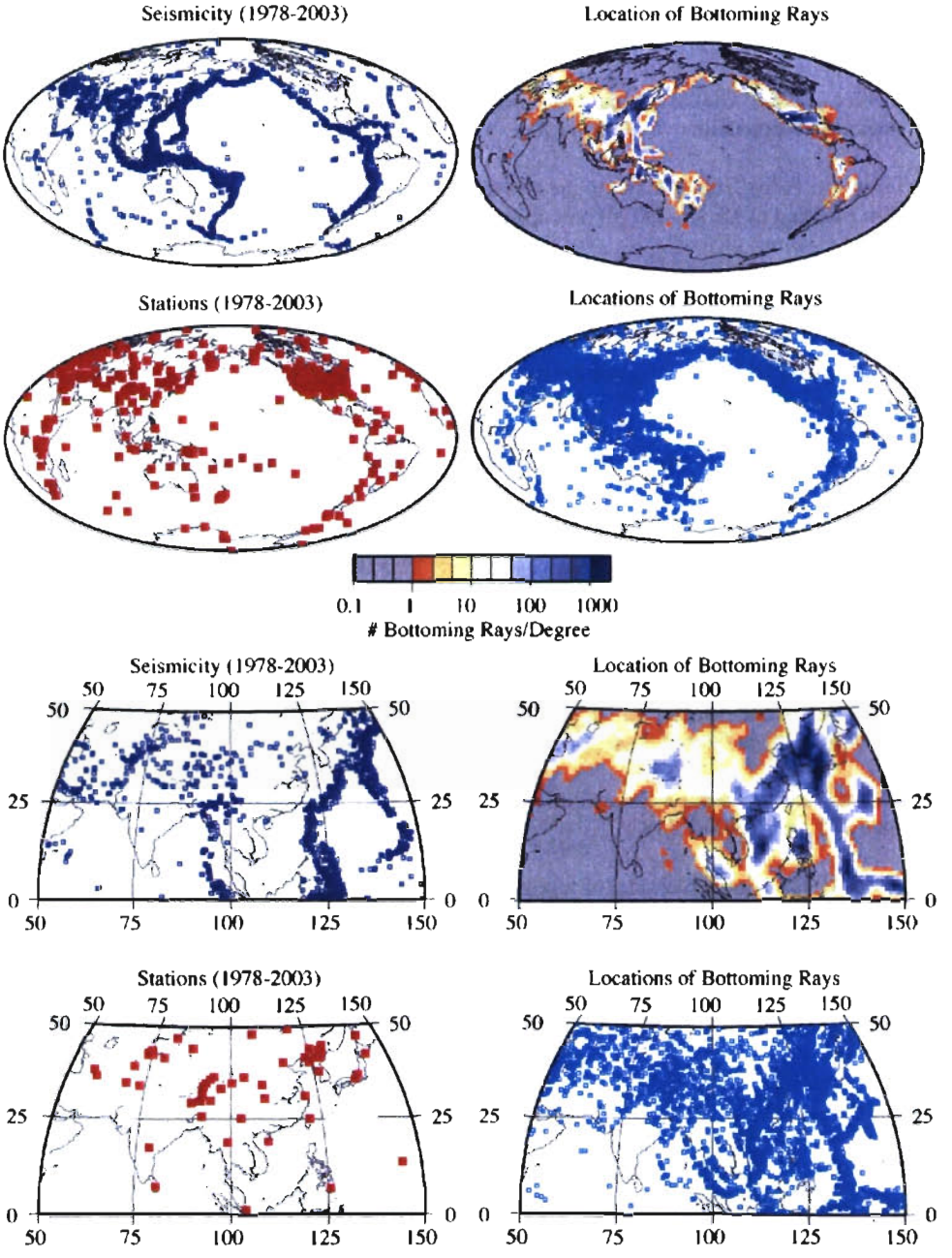

Figure 3. Seismicity and station locations for the IRIS FARM data (left panels) and midpoints of rays for source-receiver distances between 13 and 33 degrees (right panels). Global results are shown in the top four panels; regional results for Asia are shown in the bottom four panels.

REFERENCES

Chambers, K., A. Deuss, and J. H. Woodhouse (2005). Reflectivity of the 410-km discontinuity from PP and SS precursors, *J. Geophys. Res.* 110: B02301, doi:10.1029/2004JB003345.

Flanagan, M. P. and P. M. Shearer (1998a). Global mapping of topography on transition zone velocity discontinuities by stacking SS precursors, *J. Geophys Res.* 102: pp. 2,673–2,692.

Flanagan, M. P. and P. M. Shearer (1998b). Topography on the 410-km seismic velocity discontinuity near subduction zones from stacking of sS, sP, and pP precursors, *J. Geophys. Res.*:103: 21, pp. 165-21, 182.

Gu, Y., A. M. Dziewonski, and C. B. Agee (1998). Global decorrelation of the topography of transition zone discontinuities, *Earth Planet. Sci. Lett.*, Vol. 157, pp. 57–76.

Melbourne, T. and D. Helmberger (1998). Fine structure of the 410-km discontinuity, *J. Geophys. Res.* 103: pp. 10,091–10,102.

Shearer, P. M. (1990). Seismic imaging of upper-mantle structure with new evidence for a 520-km discontinuity, *Nature* 344: pp. 121–126.

Shearer, P. M. (1991). Constraints on upper-mantle discontinuities from observations of long-period reflected and converted phases, *J. Geophys. Res.* 96: pp. 18,147–18,182.

Shearer, P. M. (1993). Global mapping of upper mantle reflectors from long-period SS precursors, *Geophys. J. Int.* 115: pp. 878–904.

Shearer, P. M. (2000). Upper mantle seismic discontinuities, *in Earth's Deep Interior: Mineral Physics and Tomography from the Atomic to the Global Scale, AGU Geophysical Monograph 117*, pp. 115–131.

Shearer, P. M. and M. P. Flanagan (1999). Seismic velocity and density jumps across the 410- and 660-kilometer discontinuities, *Science* 285: pp. 1,545–1,548.

Shearer, P. M. and T. G. Masters (1992). Global mapping of topography on the 660 km discontinuity, *Nature* 355: pp. 791–796.

Veith, K. F. and G. E. Clawson (1972). Magnitude from short-period P-wave data, *Bull. Seismol. Soc. Am.* 62: pp. 435–452.